International Journal of Mechanical, Industrial and Aerospace Sciences
ISSN: 2517-9950
Vol:8, No:8, 2014

Forced Heat Transfer Convection in a Porous Channel with an Oriented Confined Jet

A. Abdedou, K. Bouhadef

Abstract**—**The present study is an analysis of the forced convection heat transfer in porous channel with an oriented jet at the inlet with uniform velocity and temperature distributions. The upper wall is insulated when the bottom one is kept at constant temperature higher than that of the fluid at the entrance. The dynamic field is analysed by the Brinkman-Forchheimer extended Darcy model and the thermal field is traduced by the energy one equation model. The numerical solution of the governing equations is obtained by using the finite volume method. The results mainly concern the effect of Reynolds number, jet angle and thermal conductivity ratio on the flow structure and local and average Nusselt numbers evolutions.

Keywords**—**Forced convection, oriented confined jet, porous media.

I. Introduction

VARIOUS techniques have been proposed to enhance heat transfer. Many researchers attach more attention to jet cooling associated with a porous medium, which is an effective method in many engineering applications such as turbine blade cooling, tempering of glass and drying technology, electronic components cooling, solar collector, insulating of building, separation process in chemical engineering, etc. Comprehensive literature survey concerned with this subject is given by Al-Sanea [1], Sahoo and Sharif ([2], [3]), Dagtekin and Oztop [4] and Sivasamy et al. [5].

Numerous researches have been conducted over the last years on heat transfer due to jet cooling in clear fluid or trough porous media. Rahimi-Esho et al [6] investigated numerically the effect and the performance of the jet flow on the forced convection heat transfer in a nanofluid confined jet. Their results show that the heat transfer is mainly affected by the Reynolds number and the geometrical aspect ratio of the jet inlet height. A detailed numerical study of symmetric twin confined turbulent slot-jet impinging obliquely on an isothermal hot surface was carried out by Sharif and Afroz [7]. They found that the impingement angle and the jet exit Reynolds number play a major role on the heat transfer. They showed that for any combination of the flow and geometric parameters, there is a critical value of impingement angle below which the flow pattern is drastically modified. Shi et al. [8] studied numerically the effect of jet-to-cross-flow mass ratio and jet angles on both local and average Nusselt numbers distributions under a semi-confined impinging slot jet at different nozzle-to-target spacing. They found that the average Nusselt number decreased with the increase of the cross flow value and the peak Nusselt number increased and shifted upstream when the jet angle changer from negative to positive values. Sivasamy et al [9] analysed numerically the effect of the bouncy on the jet impingement cooling if a constant heat flux horizontal surface is immersed in a fluid saturated porous medium. They concluded that the average Nusselt number increased by increasing Peclet number and jet width. It is also found that the average Nusselt number presents minimum values for some values of Peclet number for mixed convection conditions. A numerical study of non-Darcian effects on the mixed convection heat transfer in a metallic porous block with a confined slot jet was performed by Marafie et al. [10]. Their results show that there is a substantial increase in heat removal capability using porous block and the decrease of the porosity of the porous medium leads to the increase in the average Nusselt number.

The main objective of the present work is to study the oriented confined jet in a saturated porous medium by examining the effect of Reynolds number, jet angle, and solid to fluid thermal conductivity ratio of the porous medium on the flow pattern and heat transfer performance by examining the local and average Nusselt numbers.

II. Mathematical Formulation

The system under consideration is a two dimensional parallel plate channel filled with an isotropic and homogenous porous medium saturated with a single phase fluid. The upper and the left side walls are assumed to be impermeable and insulated. The lower wall is at constant temperature higher than the inlet fluid temperature. At this inlet, the fluid enters the channel through a confined and oriented jet characterized by an angle φ measured to the horizontal line which corresponds to the zero value of φ ($\varphi = 0$). The velocity (U_0) and temperature (Tc) distributions at the entrance are uniform and constant as shown in Fig. 1. Some assumptions are considered in order to simplify the problem: Thus the flow is two-dimensional laminar incompressible and in steady state with no internal heat generation. The buoyancy and radiation effects and viscous dissipation are neglected in comparison with the conduction and convection heat transfer effects. The thermo-physical properties of the fluid and porous medium are assumed to be constant.

A. Abdedou is with Département Du Génie Mécanique, Faculté de Génie De Construction, Université Mouloud Mammeri De TiziOuzou and with LTPMP Laboratory in the Mechanical and Process Engineering Faculty, USTHB University, BP 32, El Alia, Bab Ezzouar, Algiers, Algeria (e-mail: abdedou.azzedine@gmail.com).

K. Bouhadef is with LTPMP Laboratory in the Mechanical and Process Engineering Faculty, USTHB University, BP 32, El Alia, Bab Ezzouar, Algiers, Algeria (e-mail: kbouhadef@usthb.dz).

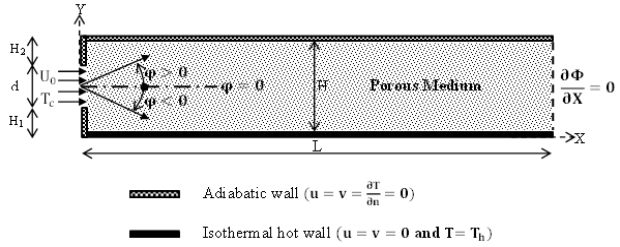

Fig. 1 Schematic diagram of the physical model and coordinate system

Under these assumptions, the dimensional governing equations that describe the flow behavior are put in dimensionless form by introducing the following dimensionless variables:

$$X = \frac{x}{H};\ = \frac{y}{H};\ U = \frac{u}{U_0};\ V = \frac{v}{U_0};\ P = \frac{p}{\rho U_0^2};\ \theta = \frac{T-T_c}{T_h-T_c} \qquad (1)$$

The dimensionless governing equations are thereby written as:

Continuity equation:

$$\frac{\partial U}{\partial X} + \frac{\partial V}{\partial Y} = 0 \qquad (2)$$

Momentum equations, in X and Y directions, based on the Brinkman- Forchheimer extended Darcy model:

$$\frac{\partial U}{\partial X} + V\frac{\partial U}{\partial X} = -\varepsilon^2\frac{\partial P}{\partial X} + \frac{\varepsilon}{Re}\left(\frac{\partial^2 U}{\partial X^2} + \frac{\partial^2 U}{\partial Y^2}\right) - \frac{\varepsilon^2}{ReDa}U - \frac{\varepsilon^2 C_F}{\sqrt{Da}}\sqrt{U^2+V^2}U \qquad (3)$$

$$U\frac{\partial V}{\partial X} + V\frac{\partial V}{\partial X} = -\varepsilon^2\frac{\partial P}{\partial Y} + \frac{\varepsilon}{Re}\left(\frac{\partial^2 V}{\partial X^2} + \frac{\partial^2 V}{\partial Y^2}\right) - \frac{\varepsilon^2}{ReDa}V - \frac{\varepsilon^2 C_F}{\sqrt{Da}}\sqrt{U^2+V^2}V \qquad (4)$$

The thermal field is modeled by the energy one equation model, when the local thermal equilibrium is assumed to be verified between the two phases ($\theta_s = \theta_f$), which leads to the following expressions:

$$U\frac{\partial \theta}{\partial X} + V\frac{\partial \theta}{\partial X} = \frac{(1-\varepsilon)R_k+\varepsilon}{RePr}\left(\frac{\partial^2 \theta}{\partial X^2} + \frac{\partial^2 \theta}{\partial Y^2}\right) \qquad (5)$$

where u, V are the longitudinal (along X direction) and transversal (along Y direction) velocity component, respectively, P is the dimensionless pressure field, $C_F$the inertial coefficient, ε the porosity of the porous medium and θ the dimensionless temperature field. In addition, the dimensionless governing parameters appearing in the above equations: the Reynolds, Darcy and Prandtl and thermal conductivity ratio are defined respectively, as:

$$Re = \frac{U_0 H}{\nu};\ Da = \frac{K}{H^2};\ Pr = \frac{\nu}{\alpha};\ \text{and}\ R_k = \frac{k_s}{k_f} \qquad (6)$$

where k_s, k_f are the solid and fluid thermal conductivities, respectively, ν is the kinematic viscosity, α is the fluid thermal diffusivity, K is the permeability of the porous medium, H is the height of the channel and $U_0$is the velocity of the fluid at the inlet.

In accordance with the problem description, the associated dimensionless boundary conditions for (2)-(5) are expressed as:

At $X = 0$ and for $H_1 < Y < H_1 + d$ (jet inlet):

$$U = \frac{u}{U_0} = \cos\varphi\ ,\ V = \frac{v}{U_0} = \sin\varphi\ \text{ and }\ \theta = 0 \qquad (7)$$

It is clear from the above boundary condition that the horizontal jet (U = 1 and V = 0) correspond to the zero value of the jet angle ($\varphi = 0$). The positive and the negative values of the jet angle ($\varphi > 0$) and ($\varphi < 0$) correspond, respectively, to the jet oriented to the upper insulated wall and the lower isothermal wall.

At $X = 0$ and for $0 < Y < H_1$ and $H_1 + d < Y < 1$:

$$U = V = \frac{\partial \theta}{\partial X} = 0 \qquad (8)$$

At Y = 0 and for $0 < X < L$ (impermeable and isotherm lower wall):

$$U = V = 0 \text{and} \theta = 1 \qquad (9)$$

At Y=1 and for $0 < X < L$ (impermeable and insulated upper wall):

$$U = V = \frac{\partial \theta}{\partial Y} = 0 \qquad (10)$$

At X=L and for $0 < Y < 1$ (channel exit):

$$\frac{\partial U}{\partial X} = \frac{\partial V}{\partial X} = \frac{\partial \theta}{\partial X} = 0 \qquad (11)$$

The physical quantities of interest in the present investigation to evaluate the heat transfer rate are predicted in terms of local and average Nusselt numbers along the hot wall. Thus the local Nusselt number (Nu)is expressed as:

$$Nu = \frac{q'' H}{(T_h-T_c)k} = -\left.\frac{\partial \theta}{\partial Y}\right|_{Y=0} \qquad (12)$$

while the average Nusselt number is:

$$Nu_{av} = \frac{1}{L}\int_0^L Nu dX \qquad (13)$$

It is worth to notice that the average Nusselt number of the lower heated wall, expressed mathematically by (13) is numerically calculated by using the Simpson's rule for integration over the whole channel length.

III. Numerical Procedure

The dimensionless governing equations with the associated boundary conditions were discretised using the control volume approach given by Patankar [11] using rectangular cells with constant mesh spacing in both directions (axial and transverse). The first order upwind scheme is applied for the convection–diffusion formulation in (2)-(5). The central differencing scheme is used for the diffusion terms of the

energy equation as well as in the momentum equation. Staggered grids which mean that the components of velocity (U and V) are stored in the staggered locations (cell faces) and scalar quantities (P, θ) are stored in the center of this volume. The SIMPLE algorithm as suggested by Patankar [11] is adopted to treat the coupling between velocity and pressure fields. The set of obtained algebraic equations are solved using a numerical algorithm based on an iterative Strongly Implicit Procedure developed by Stone [12]. The iteration process is terminated if the following condition is satisfied:

$$\max\left|\frac{\Phi_{i,j}^{m+1}-\Phi_{i,j}^{m}}{\Phi_{i,j}^{m}}\right| \leq 10^{-6} \quad (14)$$

whereΦ represents a dependent variable U, V, P, and θ. The indices i, j indicate the grid point and m denotes the iteration number. Relaxation factors above the dependent variables are employed to avoid divergence during the iteration.

Concerning the mesh refinement, to analyze the effect of the grid size on the numerical solution, various grid systems from 200x104 to 300x144 (in X- and Y- directions, respectively) are tested to compare the average Nusselt number values. The results are presented in Table I for various values of $R_k$at fixed Re= 200 and 800, Da = $10^{-2}$and $\varphi = 0$. The maximum discrepancy in the values of Nu_{av}between the grid 250 x120 and the finest one (300 x144) for all values of Re and R_k is less than 1 %. Thus, the mesh size (250 x 120) is considered good enough to generate grid independence results.

TABLE I
COMPARISON OF THE RESULTS AT DIFFERENT MESH SIZES
Da=10^{-2} and $\varphi = 0$

Re	R_k	Nu_{av}		
		200 x 104	250 x 120	300 x 144
200	1	1.9712	1.9687	1.9668
200	100	0.3826	0.3770	0.3734
800	1	3.3593	3.3404	3.3220
800	100	1.1252	1.1196	1.1158

IV. RESULTS AND DISCUSSION

The heat transfer forced convection in a horizontal channel filled with a saturated porous medium submitted to an oriented confined jet was performed. Various flow conditions and thermo physical properties of the fluid and the porous medium are considered which are expressed in a large range of dimensionless controlling parameter such as solid to fluid thermal conductivity ratio $(0.1 \leq R_k \leq 1000)$, Reynolds number $(1 \leq Re \leq 1000)$ and jet angle $(-30^{\circ} \leq \varphi \leq 30^{\circ})$. Some other parameters are kept constant. So the calculations were performed for a fixed value of Prandtl number $(Pr = 0.71)$, Darcy number $(Da = 10^{-2})$, porosity $\varepsilon = 0.9$, channel length $(L = 10)$, geometric aspect ratio which is defined as the channel height to the jet height ratio $\left(\frac{H}{d} = 4\right)$ and inertial Forchheimer coefficient $(C_F = 0.1)$.

The results are presented and discussed in terms of the streamlines, local Nusselt number and average Nusselt numbers for numerous values of the above dimensionless parameters.

Fig. 2 depicts the effect of the Reynolds number on the flow structure (streamlines) for the case of the horizontal jet ($\varphi = 0$). It is observed that for a low Reynolds number such as Re=200, one can see the development of two vortex symmetrically opposed to the jet axis. The transition from the jet flow to duct flow occurs in short longitudinal distance from the channel inlet. As the Reynolds number increases (Re=400-600) the vortex length augments consequently and the transition from the jet flow to the duct flow occurs at longer axial distance from the channel inlet. When Reynolds number takes higher values (Re=800 and 1000), it is observed that the development of the jet flow is asymmetric, the vortex near the lower hot wall becomes higher than the vortex near the insulated upper wall. It is also observed that the transition from the jet to duct flow occurs over a larger axial distance from the jet inlet. The configurations of the streamlines clearly show clearly that the jet is deviated from the horizontal direction by the increase in the dimensions and the intensity of the lower vortex due to relatively high Reynolds numbers.

Fig. 3 shows the local Nusselt number distribution of at the lower heated wall for various values of Reynolds number and a fixed value of solid to fluid conductivity ratio of 10. It is observed that for a given value of Reynolds number, the local heat transfer coefficient profile presents a maximum value which corresponds to the peak value dividing the profile into two distinct parts (ascending and descending). By examining in details the local Nusselt number profiles and by comparing the results with the corresponding streamlines distribution (as reported in Fig. 2) for each given Reynolds number, it can be seen that the increasing of the Nusselt number is started with creation of vortex and ended with stopping recirculation zones. It is worth to notice that the peak value observed on each Nu profile corresponds to the point of reattachment which is characterized by ended position of the recirculation zone. It is clear from Fig. 3 that local Nusselt number is consequently affected by the increase in the Reynolds number values which leads to the rise of the flow intensity and the recirculation zone length.

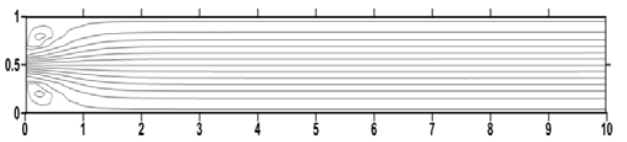

(a)

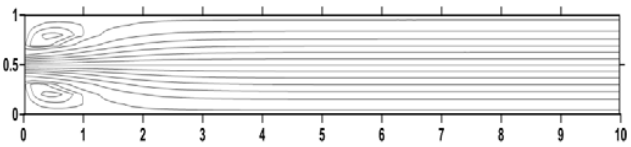

(b)

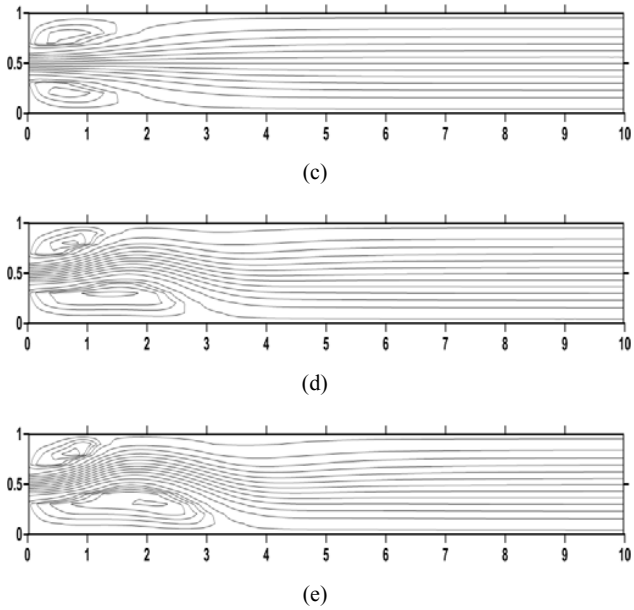

(c)

(d)

(e)

Fig. 2 Effect of Reynolds number on Streamlines for Da=10^{-2}, $\varepsilon = 0.9$ and $\varphi = 0$: (a) Re = 200; (b) Re = 400; (c) Re = 600; (d) Re = 800 and (e) Re = 1000

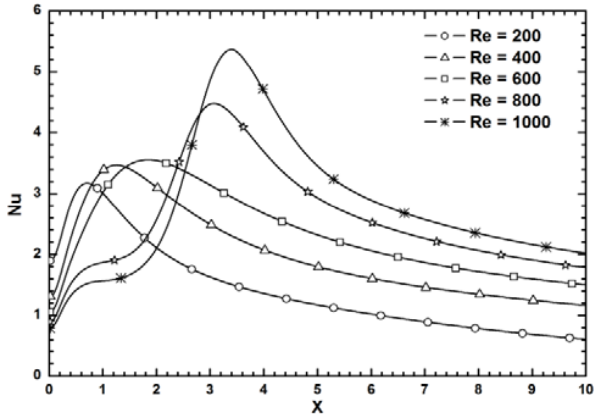

Fig. 3 Variation of the local Nusselt number with X for different values of Reynolds number at Da=10^{-2}, $\varepsilon = 0.9$, $\varphi = 0$ and $R_k = 10$

Representative streamlines plots in the flow domain for Re=1000, $\varepsilon = 0.9$ and Da=10^{-2} for three jet angles φ of -30° (jet oriented to the heated lower wall), 0° (horizontal jet) and 30° (jet oriented to the insulated upper wall) are shown in Fig. 4. It is observed in these plots that the flow domain is strongly affected by the jet angle. For a negative value of this angle (Fig. 4 (a)), one can see recirculating zones appearing in the flow domain which are separated by the main jet stream, the major one is located near the insulated upper wall and the minor one forms at the channel inlet between the stream jet and the bottom heated wall. It is clear from this plot that the main jet stream is obstructed by the formation of the third minor recirculation zone at axial distance from the channel inlet corresponding with the end of the upper major recirculation zone. This formation is the consequence of the main stream jet impingement on the bottom wall. For a jet angle value of 0° (horizontal jet), it is observed from the streamlines represented in Fig. 4 (b) that two recirculation zones develop in the flow domain. The primary major clockwise recirculation zone is formed at the channel inlet between the main stream jet and the bottom wall. A secondary minor counter-clockwise is encompassed at the channel inlet between the main stream jet and the insulated upper wall. When the jet angle takes positive value of 30°(Fig. 4 (c)), the stream jet impinges on the upper insulated wall create two distinct recirculation zones due to entrainment. It can be observed that the length of the vortex near the bottom wall is much higher than the one near the upper wall.

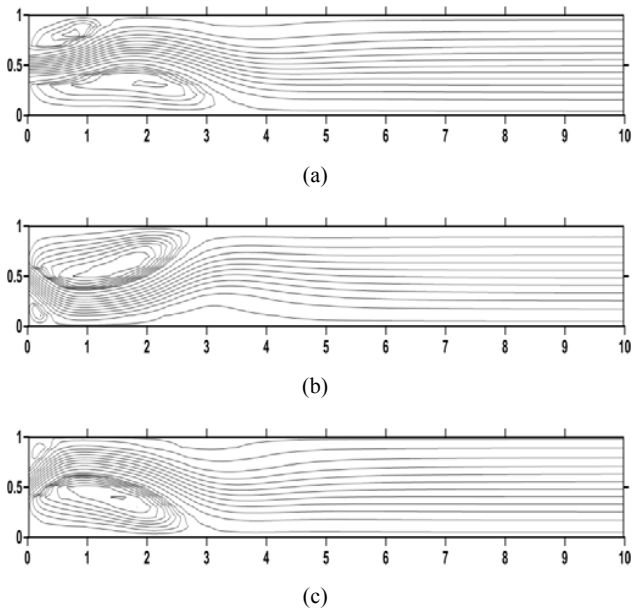

(a)

(b)

(c)

Fig. 4 Effect of jet angle on Streamlines for Da=10^{-2}, $\varepsilon = 0.9$ and Re = 1000: (a) $\varphi = -30^{o}$; (b) $\varphi = 0^{o}$ and (c) $\varphi = 30^{o}$.

Fig. 5 shows the variation of local heat transfer coefficient along the heated wall for a fixed Reynolds number value of 1000 and for various jet angle values. The general trends of these plots is that, the local Nusselt number starts with a minimum value at the channel inlet and immediately increase to reach a peak value beyond which it decreases monotonically along the channel. It is also observed that the peak value corresponding to the jet oriented to the bottom wall ($\varphi = -30^{o}$) is much higher than the others ones. This is because the convection in more vigorous at the impingement region near the heated wall at the channel inlet and becomes gradually weaker by moving to the channel outlet. Another minor peak value is observed on the same local Nusselt number profile ($\varphi = -30^{o}$) at axial position near the channel centre. This corresponds to the third recirculation zone as showed by Fig. 4 (a).

Figs. 6 and 7 indicate the average Nusselt number Nu_{av} variation at the bottom hot wall with jet angle as well as with thermal conductivity ratio for two Reynolds number values

Re=100 and Re=1000, respectively. For a weak value of Re (Fig. 6), it is observed that at a given value of thermal conductivity ratio, the average Nusselt number increase starts with a low value at negative jet angle value of (-30^o) and augments with jet angle to reach a maximum value corresponding to the horizontal jet $(\varphi = 0^o)$ beyond which the average Nusselt number decreases monotonically by about 8% for R_k=0.1 and 7% for R_k=100, with the increase of jet angle from $0^o$to 30^o. When the Reynolds number takes a high value (Fig. 7) and for low values of thermal conductivity ratio, it is noticed that the average Nusselt number starts with a maximum value for a jet angle value of (-30^o) and immediately falls to a minimum value at jet angle value of 0^o. It then rises to a secondary maximum value at $\varphi = 20^o$. The average Nusselt augments by about 14 % with the decrease of jet angle from $0^o$to -30^o. For a high value of thermal conductivity ratio, the average Nusselt number increases with the increase of jet angle to rise a maximum value at $\varphi = -5^o$ beyond which it diminishes by about 13 % with the jet angle increase from $-5^o$to 30^o.

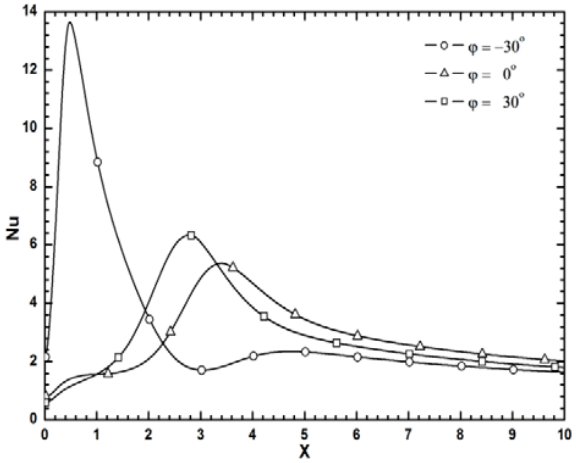

Fig. 5 Variation of the local Nusselt number with X for different values of jet angle at Da=10^{-2}, $\varepsilon = 0.9$, $\mathrm{Re} = 1000$ and $R_k = 10$.

The effect of Reynolds number on the average Nusselt number for different jet angle values as well as the thermal conductivity ratio is illustrated in Fig. 8. It is observed that the average heat coefficient increases significantly with Reynolds number more particularly for low values of thermal conductivity ratio. However, interestingly for R_k=100, the average Nusselt number remains nearly unchanged when Reynolds number increased from 1 to 100. A possible reason for this observation is that the relatively low Reynolds number associated with the high thermal conductivity of the solid in the porous medium (high R_k) leads to a small effect of convection which is less vigorous comparing to the conduction one. It can be noticed also from this figure that the effect of jet angle on the average Nusselt number depends on the Reynolds number. For a weak thermal conductivity ratio value, the average Nusselt number augments with the rise of jet angle from -30^o to 0^o at the particular Reynolds number values gap of $1 \leq \mathrm{Re} \leq 300$. This trend, however, is reversed for $\mathrm{Re} > 300$ where the average Nusselt number decreases when the jet angle augments from -30^o to 0^oas already observed in Fig. 7.

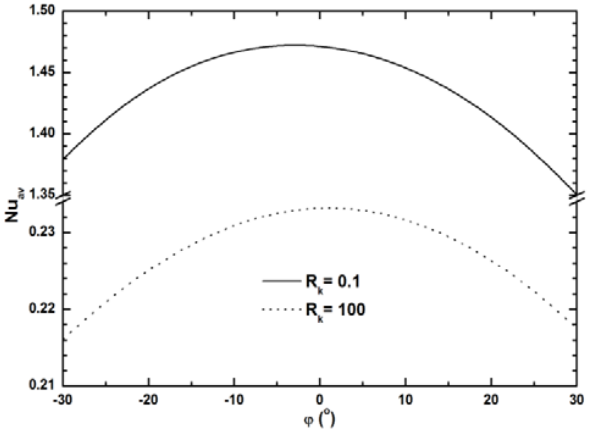

Fig. 6 Variation of the average Nusselt number with jet angle for different values of thermal conductivity ratio at Da=10^{-2}, $\varepsilon = 0.9$ and $\mathrm{Re} = 100$

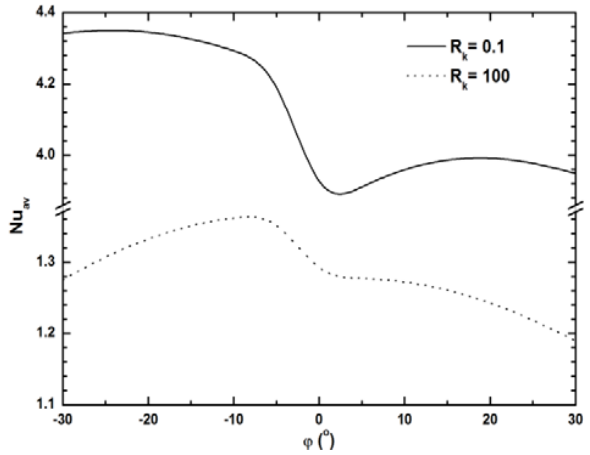

Fig. 7 Variation of the average Nusselt number with jet angle for different values of thermal conductivity ratio at Da=10^{-2}, $\varepsilon = 0.9$ and $\mathrm{Re} = 1000$

It is also of interest to investigate the effect of solid to fluid thermal conductivity ratio on the heat transfer process. The variation of the average Nusselt number with this ratio has been plotted in Fig. 9 for various values of jet angle. The general trends of these plots is that, the average Nusselt number monotonically and strongly decreases with the increase of solid to fluid conductivity ratio. The weak values of thermal conductivity ratio correspond to relatively high values working fluid thermal conductivity in comparison with the solid phase of the porous medium which allows to the fluid, in combination with the vigorous convection effects due to high Reynolds numbers, to extract more energy from the heated wall. When the thermal conductivity of the solid becomes relatively important, the heat transfer is mainly

occurred by conduction in the solid phase of the porous medium which diminishes the convection effects more particularly for low Reynolds numbers. It is also noticed that the effect of the jet angle on the average Nusselt number is affected by the thermal conductivity ratio. For high values of Re and for the gap $1 \leq R_k \leq 100$, the average Nusselt number decreases with the increase of the jet angle from -30^o to 0^o. This trend is reversed for $R_k > 100$ where the average heat exchange increases with the increase of jet angle.

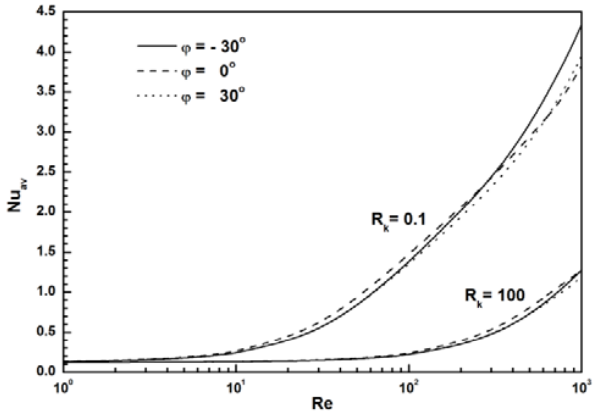

Fig. 8 Variation of the average Nusselt number with Reynolds number for different values of jet angle and thermal conductivity ratio at Da=10^{-2}, and $\varepsilon = 0.9$

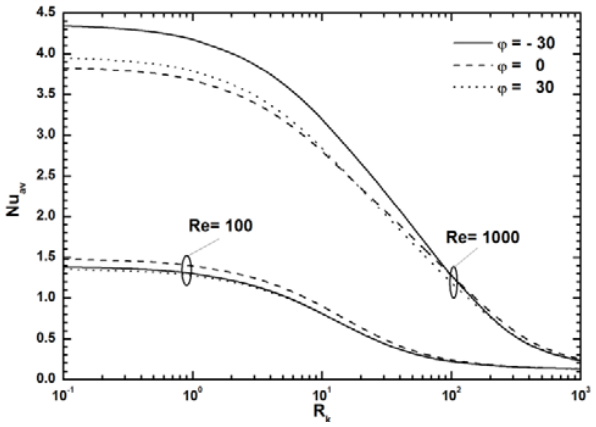

Fig. 9 Variation of the average Nusselt number with thermal conductivity ratio for different values of jet angle at Da=10^{-2} and $\varepsilon = 0.9$

V. Conclusion

Forced convection in a porous channel filled and saturated by an incompressible fluid with an oriented confined jet is numerically investigated using the finite volume method. The Brinkman-Forchheimer extended Darcy model is used to describe the fluid movement while the thermal field is modelled by the one energy equation model taking into account the local thermal equilibrium between the two fluid and solid phases. The study was conducted in the perspective to determine the effect of some geometrical and thermo physical parameters on the local and average Nusselt number at the heated wall. Analysis of the numerical results shows that flow structure is mainly affected by the Reynolds number and the jet angle. The maximum values of the average Nusselt number are obtained for high values of Reynolds number and low values of solid to fluid thermal conductivity ratio. The effect of jet angle in heat transfer enhancement is more pronounced for high Reynolds number and weak thermal conductivity ratio. Thus the average Nusselt increases by about 14 % with the decrease of jet angle from $0^o$to -30^o. The values of Reynolds number and thermal conductivity ratio of 300 and 100, respectively were found to be critical values beyond which the jet angle effect on the average Nusselt number is reversed.

References

[1] S. Al-Sanea, "A numerical study of the flow and heat transfer characteristics of an impinging laminar slot-jet including crossflow effects ," *Int. J. Heat Mass Transfer.*, vol. 35, pp. 2501–2513, 1992.

[2] D. Sahoo, M. A. R. Sharif, "Mixed convection cooling of an isothermal hot surface by confined slot jet impingement," *Num. Heat Transfer.*, vol. 45, pp. 887–909, 2004.

[3] D. Sahoo, M. A. R. Sharif, "Numerical modeling of slot-jet impingement cooling of a constant heat flux surface confined by a parallel wall," *Int. J. Thermal Sciences.*, vol. 43, pp. 877–887, 2004.

[4] I. Dagtekin, H. F. Oztop, " Heat transfer due to double laminar slot jets impingement onto an isothermal wall within one side closed long duct," *Int. J. Heat Mass Transfer.*, vol. 35, pp. 65–75, 2008.

[5] A. Sivasamy, V. Selladurai, P. R. Kanna "Mixed convection on jet impingement cooling of a constant heat flux horizontal porous layer," *Int. J . Thermal Sciences.*, vol. 49, pp. 1238–1246, 2010.

[6] M. Rahimi-Esho, A. A. Ranjbar, A. Ramiar, M. Rahgoshay "Numerical simulation of forced convection of nanofluid in a confined jet," *Heat Mass Transfer.*, vol. 48, pp. 1995–2005, 2012.

[7] F. Afroz, M. A. R Sharif, "Numerical study of heat transfer from an isothermally heated flat surface due to turbulent twin oblique confined slot-jet impingement ," *Int. J . Thermal Sciences.*, vol. 74, pp. 1–13, 2013.

[8] Y. Shi, M. B. Ray, A. S. Mujumdar "Numerical study on the effect of cross-flow on turbulent flow and heat transfer characteristics under normal and oblique semi-confined impinging slot jets," *Drying Technology.*, vol. 21, No. 10, pp. 1923–1939, 2003.

[9] A. Sivasamy, V. Selladurai, P. Rajesh Kanna "Jet impingement cooling of a constant heat flux horizontal surface in a confined porous medium: Mixed convection regime," *Int. J. Heat Mass Transfer.*, vol. 54, pp. 5847–5847, 2010.

[10] A. Marafie, K. Khanafer, B. Al-Azmi, K. Vafai, " Non-Darcian effects on the mixed convection heat transfer in a metallic porous block with a confined slot jet ," *Num. Heat Transfer.*, vol. 54, pp. 665–685, 2008.

[11] S. V. Patankar, *Numerical Heat Transfer and Fluid Flow*, Hemisphere, New York, 1980.

[12] H. L. Stone," Iterative solution of implicit approximations of multidimensional partial differential equations," *SIAM. J. Num. Anal.*, vol. 5. No. 3, September, 1968.